

PSO-based adaptive sliding mode control of a bidirectional DC-DC converter with an improved reaching law

Julius Derghe Cham¹, Francis Lénine Djanna Koffi¹, Ekemb Gabriel², Alexandre Teplaira Boum²

¹Technology and Applied Sciences Laboratory (TASL), University of Douala, Douala, Cameroon

²Department of Electrical and Electronics Engineering, ENSET, University of Douala, Douala, Cameroon

Article Info

Article history:

Received Sep 2, 2024

Revised Feb 20, 2025

Accepted Mar 1, 2025

Keywords:

Adaptive sliding mode controller

Particle swarm optimization

Reaching law

Robustness

Sliding mode controller

ABSTRACT

This paper explores the development of an adaptive sliding mode control (ASMC) that incorporates an improved optimal reaching law. We intend to use the proposed ASMC in DC microgrids and electric vehicle applications to regulate a bidirectional (two-way) buck-mode DC-DC converter. To initiate the design process, we developed a mathematical model of the converter operating in charging mode. Particle swarm optimization is employed to determine the controller's gains for better performance. By capitalizing on the benefits of the ASMC algorithm, the developed controller achieves improved reaching conditions, increased robustness, and enhanced stability. The efficacy of the suggested controller is demonstrated through MATLAB/Simulink simulations conducted on the converter, in comparison to conventional sliding mode control (CSMC) and ASMC. The comparison shows that the proposed controller achieves the intended transient response in steady-state conditions with minimal error and better reference tracking. The performance of the suggested controller is robust with respect to variations in source voltage and load resistance. For applications involving DC microgrids and electric vehicles, the suggested controller will ensure a consistent DC transit voltage.

This is an open access article under the [CC BY-SA](https://creativecommons.org/licenses/by-sa/4.0/) license.



Corresponding Author:

Julius Derghe Cham

Technology and Applied Sciences Laboratory (TASL), University of Douala

Carrefour Ange Raphaël, Douala, Cameroon

Email: julius.cham@yahoo.com

1. INTRODUCTION

Modern technology is evolving at an unprecedented pace, transforming nearly every aspect of human activity. Among these advancements, electric power plays a pivotal role, serving as the backbone for a multitude of applications across various domains. Traditionally, non-renewable sources like thermal power plants, coal, nuclear energy, and natural gas have generated electricity. While these sources have historically fueled global progress, their finite nature poses significant challenges, leading to concerns about long-term sustainability and potential shortages in the electricity supply. In the modern era, the dependence on electronic devices, particularly smartphones, underscores the critical importance of an uninterrupted power supply. A scenario devoid of electricity could force society to revert to a more traditional, disconnected way of life. Recognizing these challenges, contemporary research and technological innovation have prioritized the exploration and adoption of renewable energy sources like solar power, wind energy, and fuel cells as top priorities in light of these difficulties [1]-[5]. These renewable sources, characterized by their sustainability and lower environmental impact, produce direct current (DC) electricity. Battery storage makes it possible to use this DC power when there is excess generation or when renewable energy sources are not available. However, a key limitation of renewable energy systems is the inherent variability in power generation, which

stems from fluctuating environmental conditions. This variability poses a challenge to system reliability and necessitates the development of efficient power management systems. To address this, a two-way DC-DC converter is often employed as a critical power interface between primary renewable power sources and auxiliary energy storage systems [6]-[8]. A two-way DC-DC converter facilitates energy transfer in both directions: charging the energy storage devices when excess power is available and discharging to supply power to the load when needed. A two-way half-bridge DC-DC converter is a popular topology that is selected for this purpose. This converter acts as a power conditioning unit, ensuring smooth and efficient energy exchange between the DC bus, loads, and storage devices. To achieve this, the converter must operate within a closed-loop control system, which relies on a robust control mechanism to ensure system stability, efficiency, and responsiveness under dynamic conditions. The literature highlights a variety of control strategies applied to two-way DC-DC converters, each with its own strengths and limitations. Among these are fuzzy logic control [8], [9], model predictive control (MPC) [10]-[12], passivity-based control [13], [14], H-infinity control [15]-[17], fractional order control [18]-[20], and sliding mode control (SMC) [21]-[23]. Selecting the optimal control strategy depends on the specific application requirements, such as response time, robustness, and complexity. SMC has emerged as a particularly reliable and effective approach for power electronic converters, including two-way DC-DC converters. Numerous researchers have proposed SMC-based designs for two-way half-bridge DC-DC converters, aiming to enhance performance and address common challenges [22], [23]. Despite these advancements, existing controllers often face persistent issues, including high levels of chattering, overshooting, complex implementation, prolonged settling and rising times, and limited robustness under varying operating conditions [23]-[25].

This paper suggests a new and dependable sliding mode controller improved by particle swarm optimization (PSO) in order to get over these restrictions. This advanced control approach is designed to optimize the performance of half-bridge bidirectional DC-DC converters, making them highly suitable for applications in microgrids, electric vehicles, and charging stations. Specifically, the proposed controller aims to regulate the charging current effectively, minimizing chattering while ensuring fast response times, robustness, and efficiency. The MATLAB/Simulink software environment has been used to thoroughly examine and validate the suggested system. Simulation results illustrate how effective the improved sliding mode controller is, highlighting its ability to solve the drawbacks of current designs and satisfy the rigorous. A summary of this paper's contribution is appended as follows:

- For the two-way DC-DC converter, a proposed controller has been devised to control the DC bus voltage.
- The adaptive sliding mode controller's existence and stability have been demonstrated.
- The controller's performance has been verified by numerical simulation within the MATLAB/Simulink environment.
- It has been established that the controller is robust in the face of substantial fluctuations in source voltage, desired voltage, and load resistance.

The subsequent sections of this paper are structured as follows: i) Section 2, the two-way DC-DC converter's structure and mathematical model are explained; ii) The design of the ASMC, the SMC, and the proposed controller are treated in section 3; iii) Section 4, the simulation results for the SMC, the ASMC, and the suggested controller are compared and discussed; and iv) Section 5 provides a summary and assessment of prospects for this paper.

2. METHODOLOGY

2.1. Explanation of the suggested methodology

The goal of this research is to build an optimal control solution for a two-way DC-DC converter using a rigorous control strategy. The block diagram in Figure 1, which visually represents the methodical framework, provides a clear and intelligible summary of the complete procedure. Numerical simulations and implementations inside the MATLAB/Simulink environment are used to validate the stability and effectiveness of the proposed control systems. With the help of this simulation platform's robust and adaptable toolkit, we can model, examine, and improve intricate control systems. This enables us to thoroughly assess our suggested solutions across a range of operational circumstances. The process begins with a comprehensive computational modeling of the selected converter, accounting for its charging or step-down mode of operation considered in this study. This modeling stage is essential because it lays the groundwork for comprehending the system's dynamic behavior and determining the key elements affecting its functioning. After the modeling phase, we create the suggested controller as well as its traditional equivalents for the converter. These controllers are the result of our laborious design to solve particular problems, considering the converter's nonlinear dynamics. Optimization is the next stage following design, where the suggested controller parameters are optimized using advanced techniques such as particle swarm optimization. Finally, after comprehensive testing across a range of circumstances, the controlled system is implemented within the MATLAB/Simulink environment. By utilizing source voltage, load resistance,

desired voltage fluctuations, and white noise in both current and voltage measurements, these tests enable us to fully explore the system's capabilities.

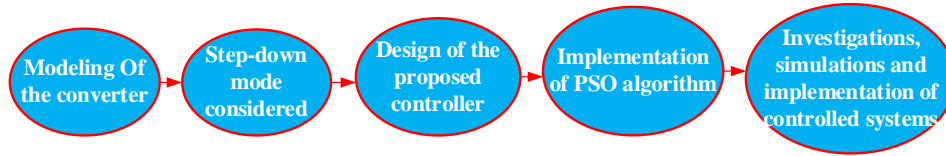


Figure 1. A description of the suggested research methods

2.2. Presentation and computational modelling of bidirectional DC-DC converter

An analogous circuit for a half-bridge two-way DC-DC converter that charges a battery is shown in Figure 2. The battery, denoted as r_L is considered an internal resistance for the purposes of this study. The battery is charged by lowering the voltage from the DC bus using a two-way DC-DC converter. Maintaining a steady DC bus voltage is the aim of a buck-mode bidirectional DC-DC converter. The indicated sources [20], [22], [23], [25] give a description of the topology of this converter. Considering that switches are complementary, that is, when one is on, the other is off, the control input can be expressed as [0, 1] when the switch is off and [1, 0] when it is on. The corresponding circuit for a two-way half-bridge DC-DC converter working in buck mode is shown in Figure 3. By using Kirchhoff's voltage and current principles, the converter's mathematical model without parasitic resistances is shown in (1) and (2).

The buck mode of a bidirectional DC-DC converter is described by the state space equations listed:

- Equation for the output when the upper switch is turned ON

$$\begin{cases} \frac{dI_L}{dt} = \frac{V_{in} - V_{C_2}}{L} \\ \frac{dV_{C_2}}{dt} = \frac{I_L}{C_2} - \frac{V_{C_2}}{r_L C_2} \\ V_{C_2} = V_o \end{cases} \quad (1)$$

- Equation for the output when the lower switch is turned ON

$$\begin{cases} \frac{dI_L}{dt} = -\frac{V_{C_2}}{L} \\ \frac{dV_{C_2}}{dt} = \frac{I_L}{C_2} - \frac{V_{C_2}}{r_L C_2} \end{cases} \quad (2)$$

We disregard the equation specifying the input since we are only concerned with managing the battery's charge and not the system's behavior. As explained in [4] and [25], the converter's average model is obtained by combining (1) and (2) to arrive at (3) using the state space averaging technique.

$$\begin{cases} \dot{x}_1 = \frac{x_1}{L} + \frac{uV_{in}}{L} \\ \dot{x}_2 = \frac{x_1}{C_2} - \frac{x_2}{r_L C_2} \end{cases} \quad (3)$$

The (3) can be represented in matrix form as defined in (4).

$$\begin{cases} \begin{bmatrix} \dot{x}_1 \\ \dot{x}_2 \end{bmatrix} = \begin{bmatrix} 0 & -\frac{1}{L} \\ \frac{1}{C_2} & -\frac{1}{r_L C_2} \end{bmatrix} \begin{bmatrix} x_1 \\ x_2 \end{bmatrix} + \begin{bmatrix} \frac{1}{L} \\ 0 \end{bmatrix} u \\ C = [0 \quad 1] \begin{bmatrix} i_L \\ V_{C_2} \end{bmatrix} \end{cases} \quad (4)$$

Where x_1 and x_2 stand for the average values. By defining the state space variables as $[x_1 \ x_2]^T = [i_L \ V_{C_2}]^T$ with u being the control signal of PWM. i.e. $u \in [0 \ 1]$ which is the duty ratio.

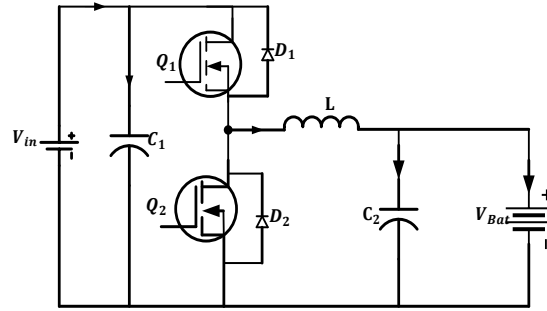


Figure 2. Bidirectional DC-DC converter

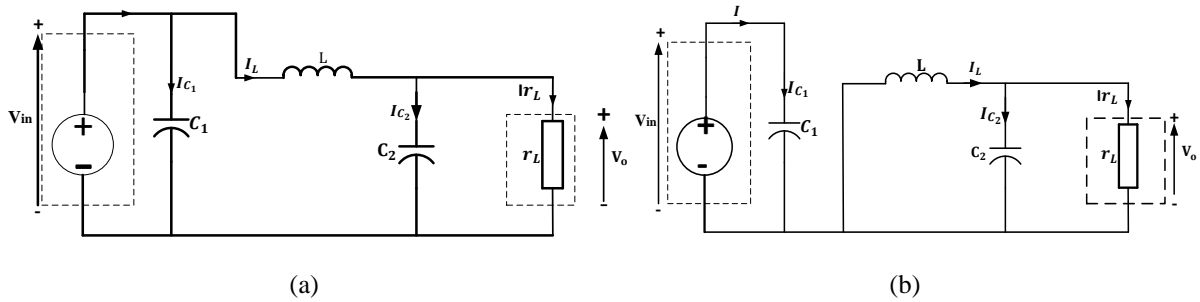


Figure 3. Equivalent circuit of a two-way half-bridge DC-DC converter in charging mode: (a) upper switch on and (b) lower switch on

2.3. Design of control techniques

2.3.1. Conventional sliding mode controller (CSMC)

When it comes to nonlinear systems like power converters, the sliding mode controller is a reliable option. It has certain noteworthy characteristics, such as robustness and accuracy [26]. With this control technique, which is a kind of variable structure control, switching control is applied at a high frequency to modify the dynamics of a nonlinear system [27]. It is a control approach intended to address modeling errors, which might manifest as parametric or unstructured uncertainties. The two main components of SMC design are the control law and the sliding surface design [28]. Because of the way it is designed, the system state must reach the designated surface, stay there, and lie in the state space. The SMC is a robust nonlinear controller that can withstand external disturbances and parameter fluctuations because it maintains the system's states on a sliding surface [23]. The (5) and [29] dictate that the sliding surface be selected as (5).

$$S = \gamma x_1 + x_2 \tag{5}$$

Where the necessary performance is gained by turning γ , a scalar. As explained in [30], the control law can be stated in (6).

$$d = \begin{cases} 1 & S > 0 \\ 0 & S < 0 \end{cases} \tag{6}$$

V_o indicates the output voltage, while V_{ref} represents the target output voltage. The (7) and (8) specify the parameters x_1, x_2 , which stand for the error and its time derivative, respectively.

$$x_1 = V_{ref} - V_o \tag{7}$$

$$\dot{x}_1 = x_2 = \frac{dx_1}{dt} = -\frac{dV_o}{dt} = -\frac{I_{C2}}{C_2} \tag{8}$$

The derivative of (5) is given by (9).

$$\dot{S} = \gamma \dot{x}_1 + \dot{x}_2 \tag{9}$$

With $x_2 = \dot{x}_1 = \frac{dV_{in}-V_o}{L}$, but $x_1 = I_L = \int \frac{dV_{in}-V_o}{L} dt$. The derivative of x_2 is presented in (10).

$$\dot{x}_2 = \frac{-dV_{in}+V_o}{LC_2} - \frac{x_2}{r_L C_2} \quad (10)$$

When (8) and (10) are entered into (9), the sliding surface's derivative is given in (11).

$$\dot{S} = \left(\gamma - \frac{1}{r_L C_2} \right) x_2 + \frac{V_o - dV_{in}}{LC_2} \quad (11)$$

Solving $\dot{S} = 0$ brings us to the equivalent control law, which is given in (12).

$$d_{eq} = \frac{LC_2}{V_{in}} \left(\gamma - \frac{1}{r_L C_2} \right) x_2 + \frac{V_o}{V_{in}} \quad (12)$$

In order to develop the control law, the system is driven to the sliding surface and kept there. The control law d is made up of two parts, which are the equivalent control (d_{eq}) and the discontinuous control (d_n) as defined in (13).

$$d = d_{eq} + d_n \quad (13)$$

With $d_n = K \text{sign}(S)$.

2.3.2. Controller for adaptive sliding mode control

The non-adaptive controller's performance is jeopardized when a rapid change in load resistance causes a disturbance. This section includes an ASMC that can react to sudden changes in load resistance to address this concern. The control law that is described here is taken from [29], [31], [32] as indicated in (14).

$$C_A = \frac{r_L}{R_d} K_n \quad (14)$$

Where $R_d \neq 0$.

$$R_d = \frac{V_o}{I_o}, \text{ with } I_o \neq 0$$

This brings the adaptive control law gain to (15).

$$C_A = \frac{I_o r_L K_n}{V_o} \quad (15)$$

Where $K_n = \gamma$ is the controller's gain and $V_o \neq 0$, r_L is the load resistance that is nominal. R_d is the instantaneous load resistance found by taking the ratio of the output voltage to the output current, which is substituted into (14), leading to (15). This gives rise to the adaptive sliding mode control law, which modifies the coefficient adaptive gain parameter (C_A) value in response to changes in load by tracking the load current. Another way to address the chattering effect is to provide a smooth hyperbolic tangent function, as shown in (16) and adopted from reference [33].

$$d_n = K \tanh(S) \quad (16)$$

As stated in [34] and defined by (17), one potential Lyapunov function ω is selected in order to guarantee circumstances around the control rule that will drive the system states to the sliding surface such that $S = 0$.

$$\omega = \frac{1}{2} S^2 \quad (17)$$

Afterwards, the temporal derivative of the aforementioned function of Lyapunov can be computed and is provided by (18).

$$\dot{\omega} = S \dot{S} \quad (18)$$

That is $\dot{\omega} < 0$. To ensure both the system's stability and the attraction of the sliding surface S , the (11) and (13) are replaced in (18) to yield $\dot{\omega} = S \left(0 - \frac{KV_i}{LC_2} \tanh(S) \right) = -\frac{SKV_i}{LC_2} \tanh(S) < 0$ with $S > 0$, where $K > 0$. By creating the nonlinear control scheme as $u_n = K \tanh(S)$, where K represents the gain and $\dot{\omega}$ is the time derivative of ω , which needs to be negatively definite, that verifies the above inequality. According to Lyapunov, the adaptive controller therefore ensures convergence and system stability.

2.3.3. Modified reaching law

Since the classical reaching law does not guarantee a finite reaching time, designing the reaching law is essential for the adaptive sliding mode controller's transient response [35]. Furthermore, a reaching law needs to be developed to regulate the movement trajectory of the system, accelerate the rate of convergence, and reduce the system's inherent chatter. In this study, an improved reaching law is applied, which is taken from [36] as stated in (19).

$$\dot{S} = -k_1 S - k_2 \operatorname{sgn}(S) \quad (19)$$

Where the additional tuning parameters $k_1 > 0$ and $k_2 > 0$ regulate the speed of convergence. A holomorphic function is substituted for the signum function in order to further reduce the chattering effect, resulting in (20).

$$\dot{S} = -k_1 S - k_2 \tanh(S) \quad (20)$$

We arrive at the overall control law defined in (21) by solving (11), (15), (16), and (20).

$$d = \frac{LC_2}{V_i} \left[\left(\frac{I_o}{V_o} r_L K_n - \frac{1}{R_L C_2} \right) x_2 + \frac{V_o}{LC_2} + k_1 S + k_2 \tanh(S) \right] \quad (21)$$

2.3.4. Optimization of particle swarms

The new optimization algorithm, known as particle swarm optimization (PSO), was first introduced by Kennedy and Eberhart and is regarded as a popular-based optimization tool. The PSO technique, which draws inspiration from flocks of birds and schools of fish (1995), uses a few simple equations to move the candidate solutions for the optimization problem, or particles, about in the search space [37], [38]. The objective function, or fitness, is the function that the optimization algorithm must minimize or maximize. The problem or function's parameter space contains a number of simple entities, or particles, each of which evaluates the fitness at its current position. Each individual in the PSO algorithm is referred to as a "particle" and is capable of moving around a multidimensional space that is a representation of the belief space. Particles retain some of their previous states because they have memory. In any case, the uniqueness of particles is preserved even if they share the same position in belief space. Individuality, the propensity to return to the particle's best prior position and sociality, or the propensity to go towards the neighborhood's best prior position are all influenced by the initial random velocity of each particle and two randomly weighted influences. Every particle attempts to alter its location by utilizing the following data:

- The present speeds
- How far the current position is from $pbest$
- How far the current location is from $gbest$
- The current position

The following are the mathematical formulas used in the search procedure as shown in (22) and (23) defined in [38] and [39]:

$$V_i^{k+1} = WV_i^k + c_1 \operatorname{rand}_1(\dots)(pbest_i - S_i^k) + c_2 \operatorname{rand}_2(\dots)(pbest_i - S_i^k) \quad (22)$$

$$S_i^{k+1} = S_i^k + V_i^{k+1} \quad (23)$$

where, V_i^k : Particle i 's speed at iteration K ; W : The weighting function; c_1, c_2 : The weighting factor is made up of randomly dispersed, uniformly distributed values between 0 and 1; $Pbest$: It is the particle's most well-known location; $gbest$: It is the Swarm's most well-known location; S_i^k : Any particle up to this point in the process has gotten the current position of the particle i at iteration k $pbest$ of particle i 's "gbest" value.

Figure 4 shows the PSO algorithm's flow chart. The steps of standard PSO algorithm are as [37]:

- Step 1: Initialize a bunch of particles by setting their speed and random position;
- Step 2: Assess each particle's fitness;

- Step 3: Compare each particle's fitness to the optimal place for their experience; and if the current location is better, update it;
- Step 4: Set a new *gbest* if it is better after comparing its suitability for each particle based on the best position *gbest* of their entire experience;
- Step 5: Modify particle position and speed using (22) and (23); and
- Step 6: Go back to step 2 if no interruptive condition is met.

The effectiveness of the suggested technique is assessed in terms of integral time absolute error (ITEA), and a variety of such criteria are offered in reference [38], [40], and defined in (24).

$$J = \int_0^T t \cdot |x_1| dt \quad (24)$$

In order to determine the ideal parameter settings for the suggested DC-DC converter control approach, the suggested method uses a PSO search. The objective function that guarantees system's stability is defined in (25) as found in [41].

$$\text{Minimise } Q(\mu) = \sum_t x_1(t)^2 \quad (25)$$

Subject to $u_b < \mu < l_b$. T is the start-up time for the transient reaction, and u_b and l_b constitute the variables' lower and upper boundaries $\mu = (\gamma, k_1, k_2)$. Consequently, PSO is used to tune and alter the gains of the proposed controller until the best time response performance is achieved. The suggested controller's schematic diagram is shown in Figure 5. In this study, a 3-x Swarm size matrix is used to estimate the position and velocity of each particle in PSO. The total number of iterations can reach 100. It is assumed that the acceleration coefficients for personal and social elements are $C_1 = C_2 = 2$. The proposed ASMC's structure is shown in Figure 5.

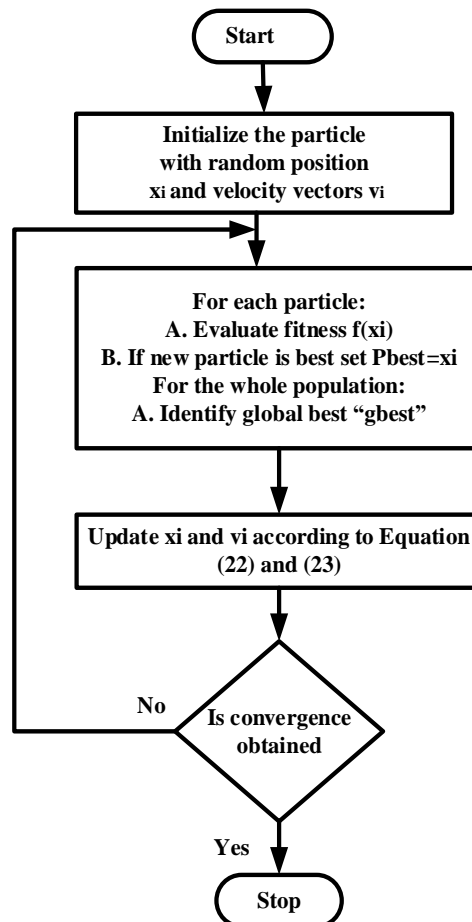


Figure 4. Particle swarm optimization algorithm

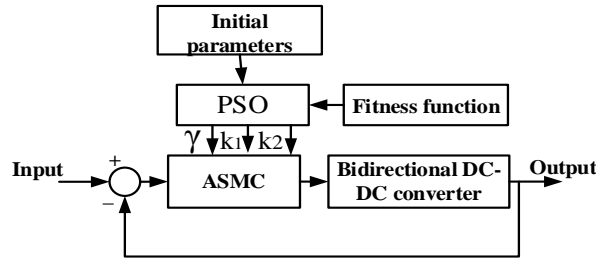


Figure 5. Design of the PSO-ASMC controller

3. RESULTS AND DISCUSSION

A numerical simulation using MATLAB/Simulink was carried out to verify the effectiveness of the recommended controller. Table 1 provides specifics on the control schemes and parameter data for the bidirectional half-bridge DC-DC converter. The sources [29], [32], and [42] were used to create these specs. Because parasitic resistances might affect the effectiveness of the system, they are included during the simulation process. Abrupt variations in the reference voltage, load resistance, input voltage, and the presence of noise in the measurement variables are used to introduce disturbances in order to judge the resilience and dynamic performance of the suggested controller.

In the first scenario, the desired output voltage is variable and changes in increments of 0.03 and 0.07 seconds, from 12 to 8 V and 10 V, respectively. The input voltage remains constant. CSMC, ASMC, and the proposed controller (ASMCRL) control the converter. It is concluded that the desired output voltage has been monitored satisfactorily by all three control strategies. Despite the abrupt change in the reference voltage, Figure 6 clearly shows that the recommended controller has a faster dynamic reaction in bringing the voltage output of the plant back to its corresponding desired values. Consequently, the suggested controller outperforms its classical counterparts in terms of control tracking accuracy. In Figure 6(a), the recommended controller is faster than its conventional techniques. Additionally, it is clear from Figure 6(b) (inductor current) that, in comparison to the traditional sliding SMC, the recommended controller lessens the chattering effect.

Table 1. Half-bridge two-way DC-DC converter and controllers' gains simulation parameters

Parameter	Value
Input voltage V_{in}	24 V
Desired output voltage V_{ref}	12 V
Switching frequency f_s	20 KHz
Inductance L	2 mH
High voltage side capacitance C_1	2400 μ F
Low voltage side capacitance C_2	47 μ F
CSMC: γ and k	3500, 0.5
ASMC: γ and k	3500, 0.5
Proposed controller: $\gamma, k_1,$ and k_2	6e3, 0.0082, 0.0037

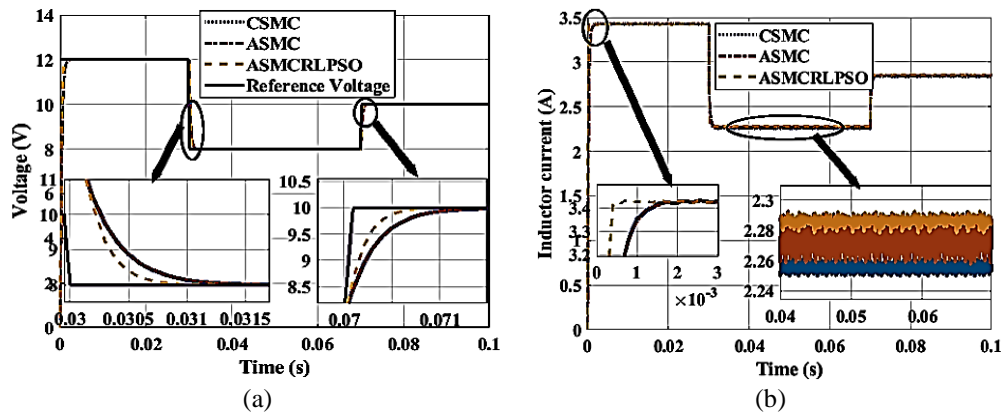


Figure 6. A comparison of the suggested controller's simulation outcomes with CSMC, and ASMC (first scenario): (a) output voltage response and (b) inductor current

The system experiences a perturbation in the second scenario due to abrupt changes in load resistance: from 3.5Ω to 1.75Ω and from 3.5Ω to 15Ω at 0.04 s and 0.05 s , respectively, with the reference voltages held constant at 12 V . The obtained results exhibit that the three control techniques performed adequately in terms of robustness, with the suggested controller demonstrating more consistent and swift performance as compared to the traditional control strategies. Nevertheless, when the load changes from 3.5Ω to 15Ω , the inductor current drops, which is referred to as under loading condition or light load. The CSMC is faster than the ASMC and the proposed controller, with a settling time of 2.1 ms as compared to 6.2 ms with the ASMC and 3.4 ms with the suggested controller. It can also be observed that the suggested controller registers a smaller overshoot and under shoot than its conventional counterparts, as shown in Tables 2 and 3. The behavior of the control strategies with regard to this change is illustrated in Figures 7 and 8 when the load suddenly changes from 3.5Ω to 1.75Ω and from 3.5Ω to 15Ω respectively. Figures 7(a) and 7(b) as well as Figures 8(a) and 8(b) represent the output voltage and inductor current, respectively.

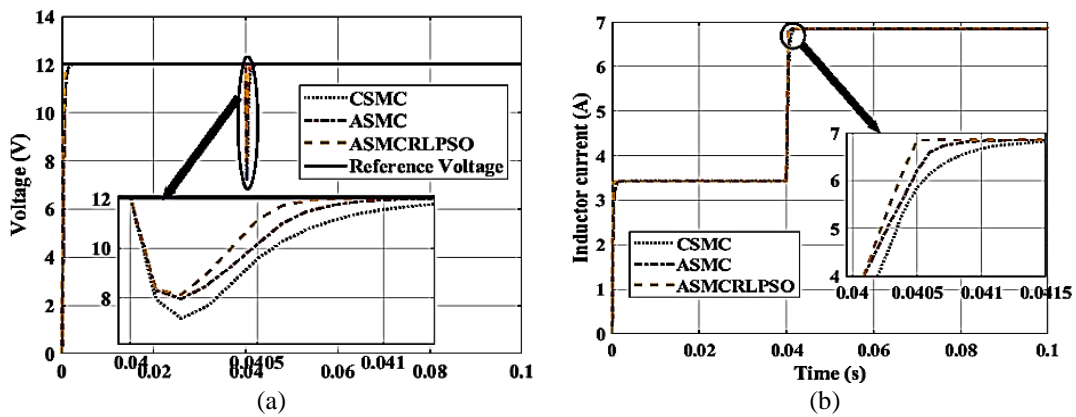


Figure 7. A comparison of the suggested controller's simulation outcomes with CSMC and ASMC (second scenario) overloading condition: (a) output voltage response and (b) inductor current

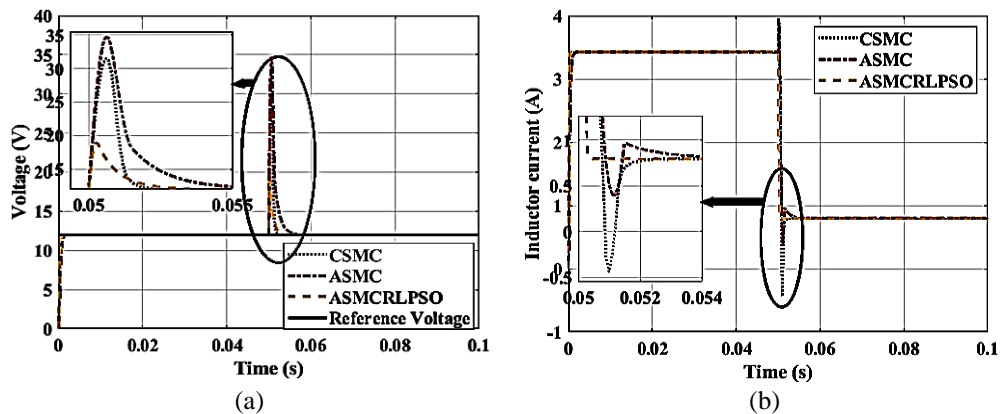


Figure 8. A comparison of the suggested controller's simulation outcomes with CSMC and ASMC (second scenario) under loading condition: (a) output voltage response and (b) inductor current

In the third scenario, the system tolerates a perturbation induced by a rapid change in input voltage from 24 V to 15 V at $t=0.03 \text{ s}$ and from 15 V to 35 V at $t=0.08 \text{ s}$, respectively, while keeping the reference voltage constant at 12 V . The results showed that both control strategies had excellent resilience, with the recommended controller outperforming the conventional control techniques in terms of speed and stability (Figure 9). In the fourth scenario, voltage and current measurement parameters are tainted with white noise to examine the potential practical performance and robustness of the proposed control scheme. This work introduces measurement noise in the form of variances of 0.14 in the measured quantities, such as voltage and current. The noise variance added to the system is depicted in Figure 10. Figures 11(a) and 11(b) illustrate the outcomes of the output voltage and inductor current measurements, respectively, when the load

changes from 3.5Ω to 1.75Ω in the presence of noise. The results of the output voltage and inductor current measurements, respectively, when the load varies from 3.5Ω to 15Ω in the presence of noise, are shown in Figures 12(a) and 12(b). The stability of the output voltage is evident despite the introduced disturbance in three control strategies, with the traditional sliding mode controller registering poor results in terms of chattering and overshoot reduction as compared to the suggested controller.

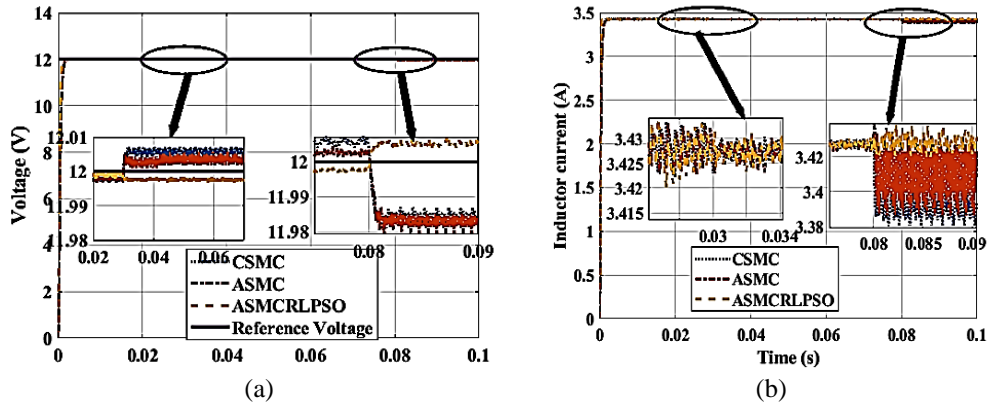


Figure 9. A comparison of the suggested controller's simulation outcomes with CSMC, and ASMC (third scenario) by varying the input voltage: (a) output voltage response and (b) inductor current

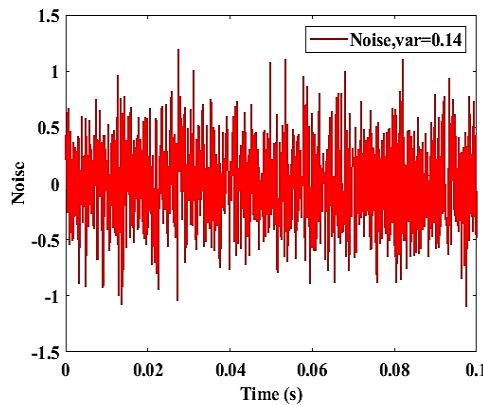


Figure 10. Magnitude of noise signal with 0.14 variance

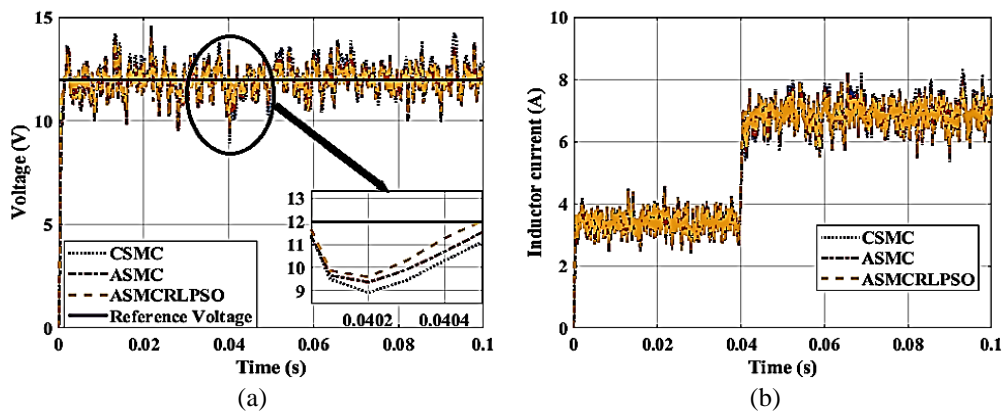


Figure 11. Comparing simulation results of the proposed controller with the classical control techniques with noise variance of 0.14 during overloading condition: (a) output voltage response and (b) inductor current

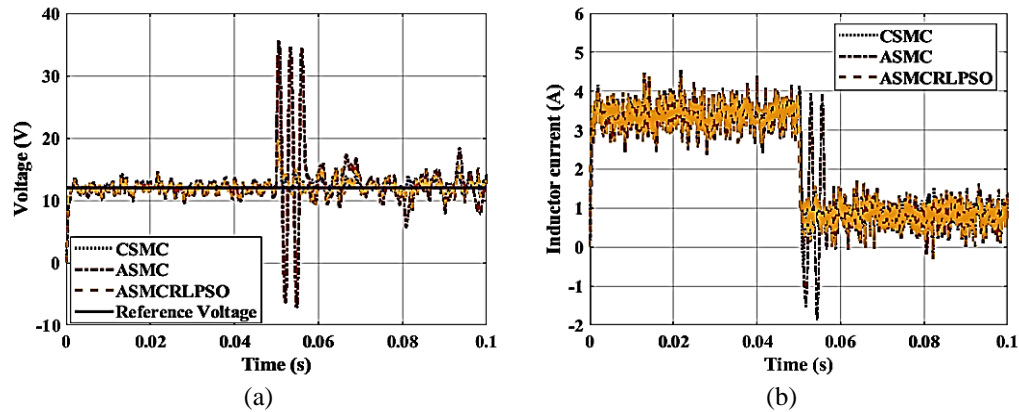


Figure 12. Comparing simulation results of the proposed controller with the classical control techniques with noise variance of 0.14 during under loading condition: (a) output voltage response and (b) inductor current

Tables 2 and 3 compare the recommended controller to the CSMC and ASMC controllers. While all three control systems achieved their goals and worked as intended, the recommended controller outperformed the other two in terms of minimum chattering, error reduction, and reference tracking. The traditional controllers present a significant overshoot and undershoot in the results, especially the ASMC during under loading conditions in the presence of noise.

Table 2. Comparison of results obtained with CSMC, ASMC, and proposed controller admits a sudden change in load resistance (from 3.5Ω to 1.75Ω) at 0.04 sec

Parameter	CSMC	ASMC	Proposed
Under overshoot (%)	40.17	33.75	32.3
Settling time (ms)	1.4	1	0.7
Rise time (ms)	0.65	0.65	0.4
IAE	0.0081	0.0074	0.0054
ISE	0.048	0.046	0.036

Table 3. Comparison of results obtained with CSMC, ASMC, and proposed controller admits a sudden change in load resistance (from 3.5Ω to 15Ω) at 0.05 sec

Parameter	CSMC	ASMC	Proposed
Peak overshoot (%)	162	189	56
Settling time (ms)	2.1	6.2	3.4
Rise time (ms)	0.65	0.65	0.4
IAE	0.022	0.035	0.01
ISE	0.28	0.44	0.057

4. CONCLUSION

The bidirectional DC-DC converter under the control of three control strategies is presented along with the detailed design steps. The effectiveness of the suggested controller over its classical counterparts is verified using the results obtained from simulation in the MATLAB/Simulink environment. Only the buck mode of operation is considered in this study. The converter working in the buck mode is represented mathematically. The proposed controller and its classical counterparts are designed and simulated within the MATLAB/Simulink environment. The simulation results illustrate that during underloading and overloading conditions, the suggested controller operates satisfactorily. Results from the simulation demonstrate that the suggested ASMC, whose gains are optimized by a PSO algorithm, gives the bidirectional DC-DC converter stable and consistent performance even when the input voltage, load resistance, and reference voltage change. In DC microgrid or electric vehicle applications, the recommended controller will ensure a constant DC transit voltage. Nevertheless, further research will be done in the future to validate the simulated results with real-time implementation.

FUNDING INFORMATION

The author(s) received no financial support for the research, authorship, and/or publication of this article.

AUTHOR CONTRIBUTIONS STATEMENT

This journal uses the Contributor Roles Taxonomy (CRediT) to recognize individual author contributions, reduce authorship disputes, and facilitate collaboration.

Name of Author	C	M	So	Va	Fo	I	R	D	O	E	Vi	Su	P	Fu
Julius Derghe Cham	✓	✓	✓	✓	✓	✓			✓	✓	✓			
Francis Lénine Djanna Koffi	✓	✓		✓	✓	✓	✓		✓	✓		✓	✓	
Ekemb Gabriel	✓	✓		✓	✓	✓		✓	✓		✓			
Alexandre Teplaira Boum	✓	✓		✓	✓	✓	✓		✓	✓	✓	✓	✓	

C : **C**onceptualization

M : **M**ethodology

So : **S**oftware

Va : **V**alidation

Fo : **F**ormal analysis

I : **I**nvestigation

R : **R**esources

D : **D**ata Curation

O : **O**riting - **O**riginal Draft

E : **E**riting - **R**eview & **E**ditng

Vi : **V**isualization

Su : **S**upervision

P : **P**roject administration

Fu : **F**unding acquisition

CONFLICT OF INTEREST STATEMENT

The authors declare that they have no known competing financial interests or personal relationships that could have appeared to influence the work reported in this paper.

DATA AVAILABILITY




The authors confirm that the data supporting the findings of this study are available within the article.

REFERENCES




- [1] V. Viswanatha and R. V. S. Reddy, "Microcontroller based bidirectional buck-boost converter for photo-voltaic power plant," *Journal of Electrical Systems and Information Technology*, vol. 5, no. 3, pp. 745–758, Dec. 2018, doi: 10.1016/j.jesit.2017.04.002.
- [2] V. Viswanatha and R. V. S. Reddy, "Digital control of buck converter using Arduino microcontroller for low power applications," in *2017 International Conference On Smart Technologies For Smart Nation (SmartTechCon)*, IEEE, Aug. 2017, pp. 439–443, doi: 10.1109/SmartTechCon.2017.8358412.
- [3] M. O. Alsumady, Y. K. Alturk, A. Dagamseh, and M. Tantawi, "Controlling of DC-DC buck converters using microcontrollers," *International Journal of Circuits, Systems and Signal Processing*, vol. 15, pp. 197–202, Mar. 2021, doi: 10.46300/9106.2021.15.22.
- [4] V. Viswanatha, R. V. S. Reddy, and Rajeswari, "Characterization of analog and digital control loops for bidirectional buck-boost converter using PID/PIDN algorithms," *Journal of Electrical Systems and Information Technology*, vol. 7, no. 1, p. 6, Dec. 2020, doi: 10.1186/s43067-020-00015-6.
- [5] V. Viswanatha and R. V. S. Reddy, "Modeling, simulation, and analysis of noninverting buck-boost converter using PSIM," in *2016 International Conference on Circuits, Controls, Communications and Computing (I4C)*, IEEE, Oct. 2016, pp. 1–5, doi: 10.1109/CIMCA.2016.8053262.
- [6] D. Ravi, B. M. Reddy, S. S.L., and P. Samuel, "Bidirectional DC to DC converters: An overview of various topologies, switching schemes and control techniques," *International Journal of Engineering & Technology*, vol. 7, no. 4.5, p. 360, Sep. 2018, doi: 10.14419/ijet.v7i4.5.20107.
- [7] A. Pathak and V. Sahu, "Review & study of bidirectional of DC-DC converter topologies for electric vehicle application," *International Journal of Science, Engineering and Technology*, vol. 3, no. 6, pp. 101–105, 2015.
- [8] M. S. Kulkarni, N. Nishikant Patil, S. Dhanaji Mane, P. R. Mane, R. Sanjay Patil, and P. Suresh Bhosale, "Design and implementation of non-isolated half bridge DC-DC bidirectional converter using fuzzy logic," 2019, [Online]. Available: <http://doi.org/10.5281/zenodo.2649929>
- [9] N. Tiwary, V. N. Naik, A. K. Panda, A. Narendra, and R. K. Lenka, "Fuzzy logic based direct power control of dual active bridge converter," in *2021 1st International Conference on Power Electronics and Energy (ICPEE)*, IEEE, Jan. 2021, pp. 1–5, doi: 10.1109/ICPEE50452.2021.9358536.
- [10] A. Pirooz and R. Noroozian, "Model predictive control of classic bidirectional DC-DC converter for battery applications," in *2016 7th Power Electronics and Drive Systems Technologies Conference (PEDSTC)*, IEEE, Feb. 2016, pp. 517–522, doi: 10.1109/PEDSTC.2016.7556914.
- [11] J. Sun and K. W. E. Cheng, "Bidirectional DC/DC converter based on the model predictive control method: Application to the Battery," in *2020 8th International Conference on Power Electronics Systems and Applications (PESA)*, IEEE, Dec. 2020, pp. 1–5, doi: 10.1109/PESA50370.2020.9344025.
- [12] Q. Xu, Y. Yan, C. Zhang, T. Dragicevic, and F. Blaabjerg, "An offset-free composite model predictive control strategy for DC/DC buck converter feeding constant power loads," *IEEE Transactions on Power Electronics*, vol. 35, no. 5, pp. 5331–5342, May 2020, doi: 10.1109/TPEL.2019.2941714.
- [13] J. Li, Y. Zhao, X. Wu, Y. Zhang, and J. Wang, "Passivity-based control of dual active bridge converter in constant power load condition," *Energies*, vol. 15, no. 18, p. 6685, Sep. 2022, doi: 10.3390/en15186685.

- [14] F. Zhang, J. Li, G. Zhu, R. Hu, Y. Qu, and Y. Zhang, "Passivity-based control of buck-boost converter for different loads research," *Journal of Electrical and Computer Engineering*, vol. 2023, pp. 1–10, Jun. 2023, doi: 10.1155/2023/5558246.
- [15] M. A. Hassans, C.-L. Su, J. Pou, D. Almakhlis, T.-S. Zhan, and K.-Y. Lo, "Robust passivity-based control for interleaved bidirectional DC–DC power converter with constant power loads in DC shipboard microgrid," *IEEE Transactions on Transportation Electrification*, vol. 10, no. 2, pp. 3590–3602, Jun. 2024, doi: 10.1109/TTE.2023.3307878.
- [16] I. Herman and M. Sebek, "Scaling of H-infinity norm in symmetric bidirectional platoons," *IFAC-PapersOnLine*, vol. 49, no. 22, pp. 91–96, 2016, doi: 10.1016/j.ifacol.2016.10.378.
- [17] V. Sundaramoorthy, S. Jeyakumar, V. Rajakumar, and V. Veerasamy, "Design of robust H2/H-infinity controllers of DC-DC SEPIC converter for effective set point tracking," *International Journal of Pure and Applied Mathematics*, vol. 118, no. 24, 2018.
- [18] L. Umasankar, H. Jayaraj, C. Rajeswaran, and M. Magesh, "Optimal fractional order PID controller design of bidirectional DC-DC converter using falcon optimization algorithm," *International Journal of Intelligent Engineering and Systems*, vol. 15, no. 3, pp. 36–48, 2022, doi: 10.22266/ijies2022.0630.04.
- [19] L. M. Martínez-Patino, J. G. Parada-Salado, F. J. Pérez-Pinal, A. G. Soriano-Sánchez, A. I. Barranco-Gutiérrez, and C. Zarate-Orduño, "Fractional-order control for voltage regulation in bidirectional converters: An experimental study," *IEEE Latin America Transactions*, vol. 22, no. 3, pp. 222–228, 2024, doi: 10.1109/TLA.2024.10431419.
- [20] C. T. Rodríguez, J. S. Choachí, and G. B. Rozo, "Fractional order control for a bidirectional converter operating in a DC," *Informador Técnico*, vol. 84, no. 1, 2019, doi: 10.23850/22565035.2387.
- [21] F. Errahimi, N. Es sbai, Z. El Idrissi, and Y. Cheddadi, "Robust integral sliding mode controller design of a bidirectional DC charger in PV-EV charging station," *International Journal of Digital Signals and Smart Systems*, vol. 5, no. 2, p. 137, 2021, doi: 10.1504/ijdsss.2021.10036181.
- [22] H. A. Trinh *et al.*, "Robust adaptive control strategy for a bidirectional DC-DC converter based on extremum seeking and sliding mode control," *Sensors*, vol. 23, no. 1, 2023, doi: 10.3390/s23010457.
- [23] S. Liu *et al.*, "Application of an improved STSMC method to the bidirectional DC–DC converter in photovoltaic DC microgrid," *Energies*, vol. 15, no. 5, 2022, doi: 10.3390/en15051636.
- [24] K. K. Mathew and D. M. Abraham, "PWM-based sliding mode current controller for bidirectional DC-DC converters in electric vehicles," *Proceedings of 2020 IEEE International Conference on Power, Instrumentation, Control and Computing, PICC 2020*, 2020, doi: 10.1109/PICC51425.2020.9362431.
- [25] L. Wang, T. Miao, X. Liu, and S. Liu, "Sliding mode control of Bi-directional DC/DC converter in DC microgrid based on exact feedback linearization," *Wseas Transactions on Circuits and Systems*, vol. 19, pp. 206–211, 2020, doi: 10.37394/23201.2020.19.23.
- [26] A. Safari and H. Ardi, "Sliding mode control of a bidirectional buck/boost DC-DC converter with constant switching frequency," *Iranian Journal of Electrical and Electronic Engineering*, vol. 14, no. 1, pp. 69–84, 2018, doi: 10.22068/IJEEE.14.1.69.
- [27] M. U. Hatlehol and M. Zadeh, "Super-twisting algorithm second-order sliding mode control of a bidirectional DC-to-DC converter supplying a constant power load," *IFAC-PapersOnLine*, vol. 55, no. 31, pp. 287–294, 2022, doi: 10.1016/j.ifacol.2022.10.444.
- [28] Y. Yin, J. Mao, and R. Liu, "Multivariable-feedback sliding-mode control of bidirectional DC/DC converter in DC microgrid for improved stability with dynamic constant power load," *Electronics (Switzerland)*, vol. 11, no. 21, 2022, doi: 10.3390/electronics11213455.
- [29] F. Tahri, A. Tahri, and S. Flazi, "Sliding mode control for DC–DC buck converter," in *Third International Conference on Power Electronics and Electrical Drives ICPEED'14At: University of science and technology of Oran*, 2014, doi: 10.13140/2.1.1857.4408.
- [30] P. Sivaraman, T. Logeswaran, J. S. S. S. Raj, and S. Boopathimanikandan, "Design and analysis of sliding mode control for battery charging applications," *IOP Conference Series: Materials Science and Engineering*, vol. 995, no. 1, p. 012002, Nov. 2020, doi: 10.1088/1757-899X/995/1/012002.
- [31] S. C. Tan, Y. M. Lai, C. K. Tse, and M. K. H. Cheung, "An adaptive sliding mode controller for buck converter in continuous conduction mode," in *Conference Proceedings - IEEE Applied Power Electronics Conference and Exposition - APEC*, IEEE, 2004, pp. 1395–1400, doi: 10.1109/APEC.2004.1296046.
- [32] G. Prasanthi and T. Anuradha, "Adaptive sliding mode control for PWM based buck converter," *International Journal of Advanced Research Trends in Engineering and Technology (IJARTET)*, vol. 2, no. 9, 2015.
- [33] G. Mustafa, F. Ahmad, R. Zhang, E. U. Haq, and M. Hussain, "Adaptive sliding mode control of buck converter feeding resistive and constant power load in DC microgrid," *Energy Reports*, vol. 9, pp. 1026–1035, Mar. 2023, doi: 10.1016/j.egy.2022.11.131.
- [34] Q. Xu, N. Vafamand, L. Chen, T. Dragicevic, L. Xie, and F. Blaabjerg, "Review on advanced control technologies for bidirectional DC/DC converters in DC microgrids," *IEEE Journal of Emerging and Selected Topics in Power Electronics*, vol. 9, no. 2, pp. 1205–1221, Apr. 2021, doi: 10.1109/JESTPE.2020.2978064.
- [35] B. Wang, C. Wang, Q. Hu, G. Ma, and J. Zhou, "Adaptive sliding mode control with enhanced optimal reaching law for boost converter based hybrid power sources in electric vehicles," *Journal of Power Electronics*, vol. 19, no. 2, pp. 549–559, 2019, doi: 10.6113/JPE.2019.19.2.549.
- [36] S. Singh, N. Rathore, and D. Fulwani, "Mitigation of negative impedance instabilities in a DC/DC buck-boost converter with composite load," *Journal of Power Electronics*, vol. 16, no. 3, pp. 1046–1055, May 2016, doi: 10.6113/JPE.2016.16.3.1046.
- [37] N. Mustafa and F. H. Hashim, "Design of a predictive PID controller using particle swarm optimization," *International Journal of Electronics and Telecommunications*, vol. 66, no. 4, pp. 737–743, Jul. 2020, doi: 10.24425/ijet.2020.134035.
- [38] A. J. Humaidi and A. F. Hasan, "Particle swarm optimization-based adaptive super-twisting sliding mode control design for 2-degree-of-freedom helicopter," *Measurement and Control*, vol. 52, no. 9–10, pp. 1403–1419, Nov. 2019, doi: 10.1177/0020294019866863.
- [39] V. V. Nagireddy, D. V. A. Kumar, and K. V. Reddy, "Optimal placement and sizing of multiple distributed generation using combined differential evaluation-HPSO method," *International Journal of Engineering and Advanced Technology (IJEAT)*, no. 1, pp. 2249–8958, 2014.
- [40] G. M. V. Gil, L. L. Rodrigues, R. S. Inomoto, A. J. Sguarezi, and R. M. Monaro, "Weighted-PSO applied to tune sliding mode plus PI controller applied to a boost converter in a PV system," *Energies*, vol. 12, no. 5, 2019, doi: 10.3390/en12050864.
- [41] S. V. Teja, T. N. Shanavas, and S. K. Patnaik, "Modified PSO based sliding-mode controller parameters for buck converter," in *2012 IEEE Students' Conference on Electrical, Electronics and Computer Science*, IEEE, Mar. 2012, pp. 1–4, doi: 10.1109/SCEECS.2012.6184759.
- [42] L. Ardhenta and T. Nurwati, "Comparison of sliding mode controller application for buck-boost converter based on linear sliding surface," *International Journal of Power Electronics and Drive Systems (IJPEDS)*, vol. 15, no. 4, p. 2397, Dec. 2024, doi: 10.11591/ijpeds.v13i1.pp423-431.




BIOGRAPHIES OF AUTHORS

Julius Derghe Cham    is a Ph.D. student in the Laboratory of Technology and Applied Science at the University of Douala. He received his Dipet 2, M.Sc., and M.Eng. degrees in Electrical Engineering from the University of Bamenda, Douala, and Buea in 2015, 2020, and 2021, respectively. His research interests include the fields of power electronics, renewable energy, artificial intelligence, and non-linear controllers. He can be contacted at email: julius.cham@yahoo.com.






Francis Lénine Djanna Koffi    is an academic researcher at the University of Douala, specializing in Environmental Science and Biomass Ecology. With a strong record of scholarly contributions, he has participated in over 30 conferences and has authored more than 30 peer-reviewed scientific publications. Djanna has also played a significant role in academic mentorship, supervising 30 Master's and 5 Ph.D. Thesis. Currently, he serves as the Head of the Division of Internships, where he is responsible for overseeing Permanent Training and fostering relationships with professional skills networks. He can be contacted at email: djannaf@yahoo.com.



Ekemb Gabriel    was born in Matomb, Cameroon. He received the B.S. and M.S. degrees in pedagogical sciences and electrical engineering and the D.E.A. degree in electrical engineering from the University of Douala, Douala, Cameroon, in 1995, 1997, and 2006, respectively. He is currently working toward the Ph.D. degree in the Université du Québec at Chicoutimi, Rouyn-Noranda, QC, Canada. From 1997 to 2003, he was a Teacher with the Technical High School, Nkongsamba, Cameroon. He joined the University of Douala as a Senior Research Associate in 2003. His research interests include high-power conversion, electromechanical interactions, and renewable energy power conversion. He can be contacted at email: ekegagaby@yahoo.fr.



Alexandre Teplaira Boum    is full professor in electrical engineering, holder of a master degree in electrical engineering and a Ph.D. in process control. His domains of interest are process control, optimization, embedded systems, smart grid, and supervisory control. He can be contacted at email: boumat2002@yahoo.fr.